

# THE EFFECT OF HYDROGEN-INDUCED SOFTENING ON THE DEFORMATION AT A CRACK TIP: IMPLICATIONS FOR FRACTURE

Y. M. Liang and P. Sofronis

Department of Theoretical and Applied Mechanics,  
University of Illinois at Urbana-Champaign,  
Urbana, IL 61801, USA

## ABSTRACT

The hydrogen concentrations in equilibrium with local stress and plastic straining are studied in conjunction with large elastic-plastic deformation in the neighborhood of a blunting crack tip. The hydrogen effect on material behavior is modeled through the hydrogen-induced volume dilatation and the reduction in the local flow stress. Plane strain finite element analysis shows that stress relaxation due to solute hydrogen decreases the extend of plastic yielding whereas hydrogen-induced material softening causes the deformation to center in the region directly ahead of the crack tip. The consequence of this result on the hydrogen-induced fracture processes is discussed.

## KEYWORDS

Hydrogen, diffusion, plasticity, softening, fracture

## INTRODUCTION

Of the many suggestions for the explanation of the hydrogen related failures, the mechanism of *hydrogen-enhanced localized plasticity (HELP)* appears to be a viable one [1]. Arguments in support of the HELP mechanism are based on experimental observations [2] and theoretical calculations [3] that in a range of temperatures and strain rates, the presence of hydrogen in solid solution decreases the barriers to dislocation motion, thereby increasing the amount of deformation that occurs in a localized region adjacent to the fracture surface [4]. The underlying principle in the HELP mechanism is the shielding of the elastic interactions between dislocations and obstacles by the hydrogen solutes [2, 3]. Reduction of the interaction energies between elastic stress centers results in enhanced dislocation mobility, i.e., decreased material local flow stress [4].

Nonetheless, significant issues remain to be resolved. Among these are: i) what is the detailed mechanism by which the enhanced dislocation mobility causes fracture in bulk specimens? ii) does the fracture occur by microvoid coalescence, formation of a Stroh crack or some other mechanism? iii) can the contribution of the plastic deformation to the fracture energy be established as a function of the hydrogen concentration? In view

of these questions, the prime goal of this paper is to address the effect of hydrogen-induced softening on the stress and deformation fields around a blunting crack tip. In a continuum sense material softening can be described through a local flow stress that decreases with increasing hydrogen concentration. It is important to emphasize that the term “flow stress” denotes the intrinsic flow characteristics of a small volume of material at the microscale around a crack tip where hydrogen concentrates as the material deforms. The amount of hydrogen concentration in the specimen is calculated by considering the effect of plastic straining (trapped hydrogen) and hydrostatic stress (normal interstitial lattice site hydrogen). In view of the very high mobility of the hydrogen solute, hydrogen concentration in trapping sites is assumed always in equilibrium with hydrogen in interstitial sites, which is also assumed to be in equilibrium with local hydrostatic stress. The calculated total hydrogen concentration is then used to estimate the material softening along the lines proposed in the work of Sofronis *et al.* [5] on the basis of the experimental observations of Tabata and Birnbuam [6]. It is emphasized that the present equilibrium calculation of the hydrogen concentrations, stress, and deformation fields is fully coupled. It should also be pointed out that the numerical predictions for our chosen model system, i.e. niobium, turn out to be independent of the amount of trapped hydrogen. Therefore, the present numerical results can be considered as an assessment of the synergism between the local hydrostatic stress and hydrogen-induced softening ahead of a crack tip. However, in view of the generality of the present approach, the current treatment can be easily applied to other systems with different trapping characteristics.

## HYDROGEN CONCENTRATION AND CONSTITUTIVE LAW

Hydrogen is assumed to reside either at normal interstitial lattice sites (NILS) or reversible trapping sites at microstructural defects generated by plastic deformation. Hydrogen concentration in NILS is studied under equilibrium conditions with local stress  $\sigma_{ij}$ , and the occupancy of NILS sites,  $\theta_L$ , is calculated through the Fermi-Dirac form in terms of the stress-free lattice concentration  $c_0$  and stress [5]. Hydrogen atoms at trapping sites are assumed to be always in equilibrium with those at NILS according to Oriani's theory [7], and the trapping site occupancy is given by  $\theta_T = \theta_L K / (1 - \theta_L + \theta_L K)$ , where  $K = \exp(W_B / RT)$ ,  $W_B$  is the trap binding energy,  $R$  is the gas constant, and  $T$  is the temperature. Thus the total hydrogen concentration (in trapping and NILS) measured in hydrogen atoms per solvent atom (H/M) is calculated as  $c = \beta \theta_L (\sigma_{kk}) + \alpha \theta_T (\theta_L) N_T (\varepsilon^P) / N_L$ , where  $N_T$  is the trap density which is a function of the effective plastic strain  $\varepsilon^P$ ,  $N_L$  is the number of host metal atoms per unit volume, and  $\alpha$ ,  $\beta$  are material constants.

Sofronis *et al.* [5] based on the calculations of Sofronis and Birnbaum [3] and on microscopic studies of the effect of hydrogen on dislocation behavior in iron [6] argued that a continuum description of the hydrogen effect on the local flow stress  $\sigma_Y$  can be stated as  $\sigma_Y = \sigma_0^H (1 + \varepsilon^P / \varepsilon_0)^{1/n}$ , where  $\sigma_0^H$  is the initial yield stress in the presence of hydrogen that decreases with increasing hydrogen concentration,  $\varepsilon_0$  is the initial yield strain in the absence of hydrogen, and  $n$  is the hardening exponent that is assumed unaffected by hydrogen. In this equation, the hydrogen effect on the local continuum flow characteristics is modeled through the initial yield stress which is assumed to be given by  $\sigma_0^H = \phi(c) \sigma_0$ , where  $\phi(c)$  is a monotonically decreasing function of the local hydrogen concentration  $c$  and  $\sigma_0$  is the initial yield stress in the absence of hydrogen. A possible suggestion for  $\phi(c)$  is a linear form  $\phi(c) = (\xi - 1)c + 1$ , where the parameter  $\xi$  which is less than 1 denotes the ratio of the yield stress in the presence of hydrogen,  $\sigma_0^H$ , to that in the absence of hydrogen,  $\sigma_0$ , at the maximum hydrogen concentration of 1.

The total deformation rate tensor (symmetric part of the velocity gradient in spatial coordinates) is written as the sum of an elastic part (which is modeled as hypo-elastic, linear and isotropic), a part due to the presence of hydrogen, and a plastic part:  $D_{ij} = D_{ij}^e + D_{ij}^h + D_{ij}^p$ . The mechanical effect of the hydrogen solute atom is purely dilatational and is phrased in terms of the deformation rate tensor as  $D_{ij}^h = \Lambda(c) \dot{c} \delta_{ij} / 3$ , where  $\dot{c}$  is the time rate of change of concentration  $c$ ,  $\Lambda(c) = \lambda / [1 + \lambda(c - c_0) / 3]$ ,  $\lambda = \Delta v / \Omega$ ,  $\Delta v$  is the volume change per atom of

hydrogen introduced into solution that is directly related to the partial molar volume of hydrogen  $V_H = \Delta v N_A$  in solution,  $\Omega$  is the mean atomic volume of the host metal atom,  $c_0$  is the corresponding initial concentration in the absence of stress, and  $\delta_{ij}$  is the Kronecker delta. The material is assumed to be rate independent, flow according to the von Mises  $J_2$  flow theory, and harden isotropically under plastic straining. Thus,

$$D_{ij}^p = \frac{1}{h} \left( \frac{3\sigma'_{kl}}{2\sigma_e} + \mu \delta_{km} \delta_{lm} \right) \frac{3\sigma'_{ij} \overset{\nabla}{\sigma}_{kl}}{2\sigma_e} \quad (1)$$

where  $\sigma_e = (3\sigma'_{ij}\sigma'_{ij}/2)^{1/2}$  is the von Mises equivalent stress,  $\sigma'_{ij} = \sigma_{ij} - \sigma_{kk}\delta_{ij}/3$  is the deviatoric stress,  $h = \frac{\partial\sigma_Y}{\partial\varepsilon^p} + \frac{\partial\sigma_Y}{\partial c} \frac{\partial c}{\partial\varepsilon^p}$ ,  $\mu = -\frac{\partial\sigma_Y}{\partial c} \frac{\partial c}{\partial\sigma_{kk}}$ ,  $\varepsilon^p = \int \sqrt{2D_{ij}^p D_{ij}^p / 3} dt$  is the effective plastic strain, and the superposed  $\nabla$  denotes the Jaumann stress rate that is spin invariant.

## NUMERICAL RESULTS

Solutions to the boundary value problem for the equilibrium hydrogen concentration coupled with material elastoplasticity are presented in the neighborhood of a blunting crack tip under plane strain mode I opening. Small scale yielding conditions were assumed and the system's temperature was 300K. The material used in the simulations was niobium, as this metal is a high H solubility system, suffers from embrittlement at room temperature, and experimental data are readily available. Displacement boundary conditions of the singular linear elastic field were imposed at a circular boundary at a distance  $L = 15\text{cm}$  from the tip. The ratio of  $L/b_0$ , where  $b_0$  is the initial crack opening displacement, was taken equal to 30,000. The finite element mesh is described in the work of Sofronis and McMeeking [8]. Before the application of the external load, the specimen was assumed to be stress free and at a uniform initial hydrogen concentration  $c_0$ . Upon loading, uniform redistribution of the H solute occurs within the solid so that hydrogen is always under quasi-static "local equilibrium" conditions with local stress and plastic strain as discussed in the previous section. Since hydrogen is assumed to be provided by a chemical reservoir, an arrangement corresponding to "far field concentration" kept constant at  $c_0$ , the calculation corresponds to a constant chemical potential for the hydrogen solute. Hydrogen was assumed to expand the lattice isotropically and its partial molar volume in solution was  $V_H = 1.88\text{cm}^3/\text{mole}$  which corresponds to  $\lambda = 0.174$ . The molar volume of niobium was  $10.852 \times 10^{-6}\text{m}^3/\text{mole}$  which implies that the number of the available NILS was  $N_L = 5.55 \times 10^{28}$  solvent lattice atoms per  $\text{m}^3$ . The hydrogen trap sites were associated with dislocations in the deforming metal. Assuming one trap site per atomic plane threaded by a dislocation, one finds that the trap site density in traps per cubic meter is given by  $N_T = \sqrt{2}\rho/a$ , where  $\rho$  is the dislocation density and  $a$  is the lattice parameter. The dislocation density  $\rho$ , measured in dislocation line length per cubic meter was considered to vary linearly with logarithmic plastic strain  $\varepsilon^p$  so that  $\rho = \rho_0 + \gamma\varepsilon^p$  for  $\varepsilon^p < 0.5$  and  $\rho = 10^{16}$  for  $\varepsilon^p \geq 0.5$ . The parameter  $\rho_0 = 10^{10}$  line length/ $\text{m}^3$  denotes the dislocation density for the annealed material and  $\gamma = 2.0 \times 10^{16}$  line length/ $\text{m}^3$ . The trap binding energy was taken equal to  $W_B = 29.2\text{kJ}/\text{mole}$  [5], the parameter  $\beta$  was set equal to 1 and this corresponds to a maximum NILS concentration of 1 H atom per solvent lattice atom, and the parameter  $\alpha$  was also set equal to 1 which denotes 1 trapping site per trap. The lattice parameter was  $a = 3.3 \times 10^{-10}\text{m}$ , Poisson's ratio  $\nu = 0.34$ , Young's modulus  $E = 115\text{GPa}$ , the yield stress in the absence of hydrogen  $\sigma_0 = 400\text{MPa}$ , the hardening coefficient  $n = 10$ , and the softening parameter  $\xi$  was set equal to 0.1.

In Figure 1, the normalized stress  $\sigma_{22}/\sigma_0$  and normalized hydrogen concentration  $c/c_0$  are plotted against normalized distance  $R/b$  from the crack tip along the axis of symmetry at an initial hydrogen concentration  $c_0 = 0.1\text{H}/\text{M}$ .

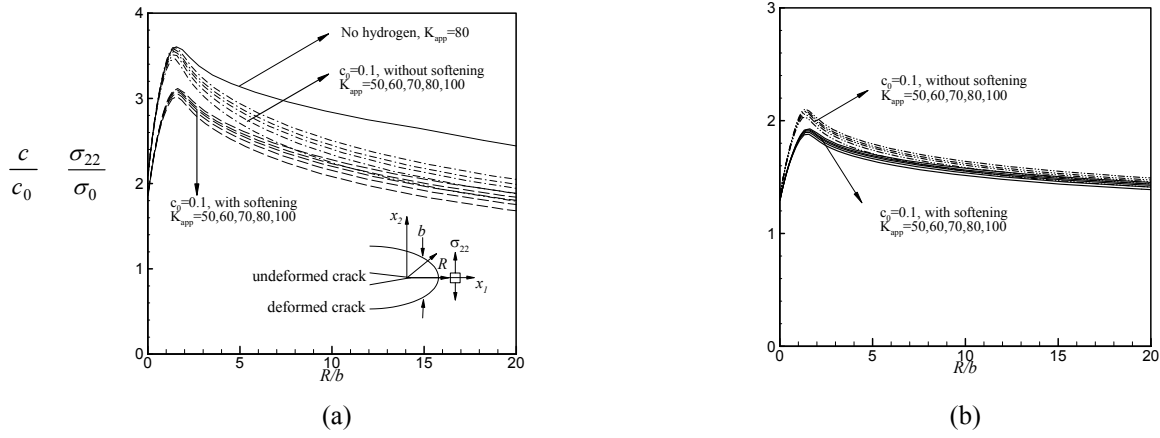


**Figure 1.** (a) plot of the normalized stress  $\sigma_{22}/\sigma_0$  vs normalized distance  $R/b$  along the axis of symmetry ahead of the crack tip for various applied stress intensities measured in  $MPa\sqrt{m}$ . The parameter  $R$  denotes the distance of a point from the notch root in the undeformed configuration and  $b$  is the current crack opening displacement; (b) plot of the normalized hydrogen concentration  $c/c_0$  vs normalized distance  $R/b$ .

Clearly, at a given initial hydrogen concentration  $c_0$ , the hydrogen concentration profiles are shown in Fig. 1b to scale with the applied load in accordance with the formula  $c = c(\sigma_{kk}, \varepsilon^p)$  and the well known corresponding scaling [9] of the stress and effective plastic strain in the small scale yielding solution. Lattice dilatation by H is accompanied with stress relaxation in the area ahead of the tip. As shown in Fig. 1a, this relaxation is more pronounced in the region  $R/b > 1.6$  where the plastic strain in the absence of hydrogen is small in comparison to the plastic strain in the region close to the crack tip ( $R/b < 1.6$ ). Hydrogen-induced softening decreases the local flow stress ahead of the crack tip, thus resulting in a reduced hydrostatic stress (Fig. 1a) and increased plastic strain. Since the hydrogen concentration profiles are dominated by the hydrostatic stress, the hydrogen concentration profile ahead of the tip is lower for a material undergoing softening due to hydrogen than for a material in the absence of any softening effect (Fig. 1a). It should also be mentioned here that the reduced hydrogen populations in the softened material are associated with a stronger stress relaxation than in the material without softening under the same applied load. Thus, the overall stress relaxation ahead of a crack tip is dictated by the synergism between material softening and relaxation due to hydrogen-induced dilatation.

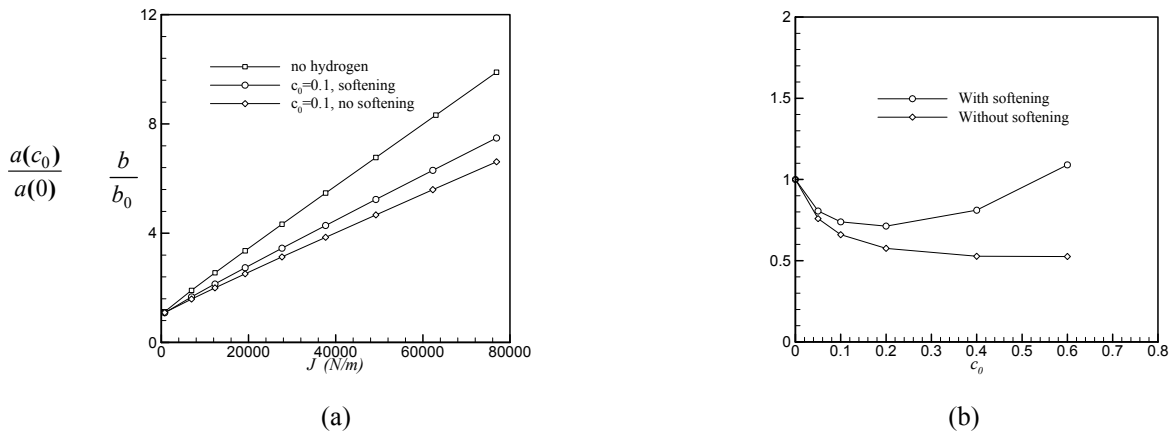


**Figure 2:** (a) Plot of normalized crack opening displacement  $b/b_0$  against the applied  $J = (1-\nu^2)K_{app}^2/E$  integral. The parameter  $b_0$  denotes the crack opening displacement in the undeformed configuration; (b) Plot of  $a(c_0)/a(0)$  against the initial hydrogen concentration  $c_0$ , where  $a(c)$  is defined through  $b/b_0 = a(c)J + 1$

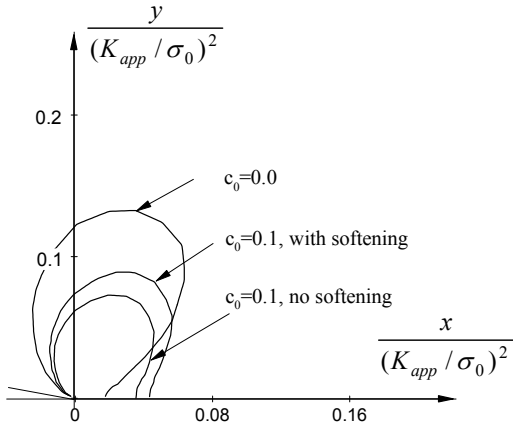


**Figure 3:** Superposed plastic zones ahead of a crack tip: for the hydrogen free material,  $c_0 = 0.1$  and with no softening, and  $c_0 = 0.1$  and with softening.

In the absence of hydrogen, there exists a linear relationship between the crack tip opening displacement (CTOD) and the applied  $J$  integral, namely  $b/b_0 = aJ + 1$  [9], where  $a$  is a constant. In the presence of hydrogen, the numerical results of Fig. 2a show that for both hydrogen-induced softening and in the absence of any softening effect, this linear relationship between  $b$  and  $J$  continues to hold. This is a direct consequence of the fact that scaling of the stress and deformation fields ahead of the tip with the applied load continues to hold in the present case of equilibrium hydrogen concentrations. Figure 2a shows that at a certain applied load and initial hydrogen concentration, hydrogen tends to close the crack, i.e., decrease the parameter  $a$ . This is because hydrogen-induced lattice dilatation relaxes the stresses around the crack tip, thus leading to reduced plastic strains behind the tip and smaller plastic zones (see Fig. 3). Furthermore, hydrogen-induced softening causes  $a$  to be greater than that without softening because the plastic zone and strains are larger in the former case than in the latter (Fig. 3). It can be

deduced that softening increases the parameter  $a$  (i.e. increases the CTOD) whereas relaxation due to dilatation decreases (i.e. decreases the CTOD) it. Also, comparing the cases with no hydrogen and hydrogen-induced softening, one sees that the softening effect is overridden by the relaxation effect at the concentration of 0.1 H/M as shown in Fig. 2a.

The dependence of the parameter  $a$  (i.e., the CTOD) on the initial hydrogen concentration  $c_0$  is shown in Fig. 2b for the cases with and without hydrogen-induced softening. For the case without softening,  $a$  decreases with increasing  $c_0$  and asymptotes a nearly constant value at large initial hydrogen concentrations. This is because for  $0 < c_0 < 0.4$ , numerical results show that the hydrogen concentration enhancement  $\Delta c = c - c_0$  ahead of the crack tip increases with  $c_0$ , thereby resulting in increased stress relaxation and in turn, in decreasing  $a(c_0)/a(0)$  (CTOD) with increasing  $c_0$ . However, for initial concentrations  $0.4 < c_0 < 0.6$ ,  $\Delta c$  is almost insensitive to  $c_0$ , in particular for  $R/b > 20$ , and hence  $a(c_0)/a(0)$  is nearly constant.

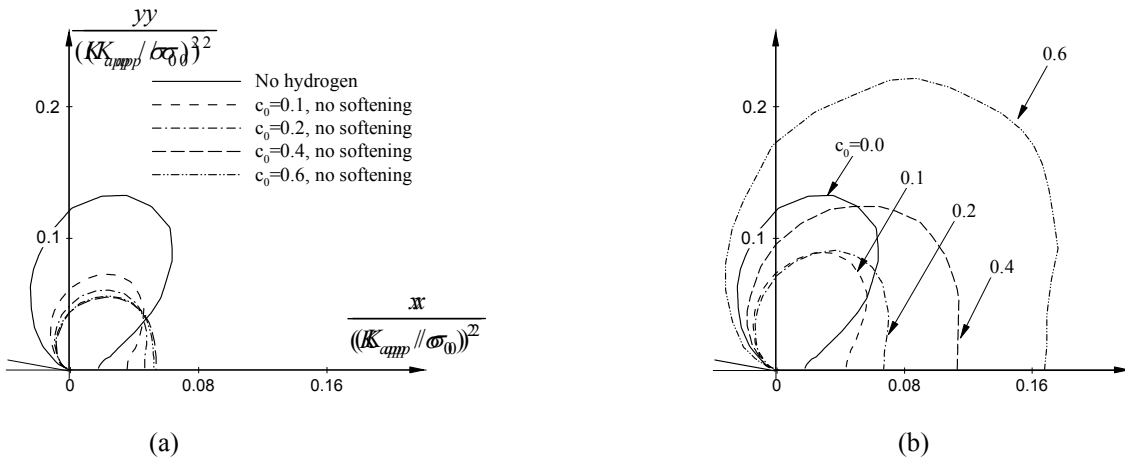


**Figure 4:** (a) Superposed plastic zones ahead of the crack tip at various initial hydrogen concentrations  $c_0$  for the case (a) without softening; and (b) with softening.

In the case of hydrogen-induced softening and  $c_0 \leq 0.2$ ,  $a(c_0)/a(0)$  decreases with increasing  $c_0$  because the relaxation due to  $\Delta c = c - c_0$  overrides the relatively small softening effect associated with concentrations  $c_0 < 0.2$ . In contrast, for  $c_0 > 0.2$  the corresponding relaxation is mild due to the small increases in  $\Delta c$ , and

this mild relaxation is overridden by the strong softening effect associated with these large initial concentrations.

The numerical results for the effect of hydrogen on the shape and size of the plastic zone in the neighborhood of the crack tip are shown in Fig. 4. First, hydrogen-induced lattice dilatation relaxes the stresses ahead of the tip and as a result, the plastic zones are shown spread and confined directly ahead of the tip and smaller (Fig. 4a) than in the absence of hydrogen. In the case of no-softening, Figure 4a shows that as the initial hydrogen concentration increases, the plastic flow of the material continues to concentrate in the region ahead of the crack tip while the plastic zone shrinks in the directions along the normal to the axis of symmetry and behind the crack tip. Shrinking of the plastic zone behind the crack tip with increasing initial hydrogen concentration (Fig. 4a) yields reduced crack opening displacements in agreement with the trend shown in Fig. 2b. For  $c_0 = 0.4$  and  $c_0 = 0.6$ , both the plastic zone shape and size are almost the same (Fig. 4a), and this also corresponds to the nearly constant  $a(c_0)/a(0)$  shown in Fig. 2b in the absence of softening. In the presence of hydrogen-induced softening, the plastic zones are shown expanding in every direction relative to the case with no softening (Figs. 3, 4b) as the initial concentration increases. Since  $c_0 = 0.1$  is a relatively low initial concentration at which the softening effect on spreading the plasticity is dominated by the local expansion and confinement of the plastic flow ahead of the tip due to the dilatation-induced relaxation, the plastic zone size continues to be smaller than that in the absence of hydrogen (Fig. 3). However, at much larger initial concentrations (e.g.  $c_0 = 0.6$ ), the softening effect results in much larger plastically deforming regions (Fig. 4b) and this is in accordance with the behavior of  $a(c_0)$  shown in Fig. 2b.

## CONCLUDING DISCUSSION

The present finite element calculations of coupled elastoplasticity with hydrogen concentration development in equilibrium with local stress and plastic strain show that that hydrogen concentration profiles ahead of a crack tip scale with the applied load for both hydrogen-induced softening and with no softening effects (Fig. 1). Dilatation-induced relaxation causes the plastic zone to expand and be confined ahead of the crack while it shrinks in all other directions. This reduces the crack tip opening displacement. In contrast, hydrogen-induced softening causes the plastic zone to expand in all directions and the CTOD to increase. At small initial concentrations ( $c_0 < 0.2$ ), stress relaxation dominates whereas softening prevails at larger initial concentrations ( $c_0 \geq 0.2$ ). As a result, the plastic zones are smaller in the former case than in the latter. However, in all cases, there is substantial plastic flow that takes place directly ahead of the crack tip which is not the case in the hydrogen free material (Fig. 4b). Therefore, one may identify the role of hydrogen with promoting intensification of the ductile fracture processes (e.g. void opening and inter-void ligament fracture by shear localization) that occur directly ahead of the crack tip. This is particularly true at small  $c_0$  ( $\sim 0.1H/M$ ) at which the hydrostatic stress, assisting void growth, is not substantially relaxed even in the case with softening.

## ACKNOWLEDGEMENTS

This work was supported by NASA through grant NAG 8-1751.

## REFERENCES

1. Birnbaum, H.K. and Sofronis, P. (1994) *Mater. Sci. & Eng.* A176, 191.
2. Sirois, E. and Birnbaum, H.K. (1992) *Acta Metall.* 40, 1377.
3. Sofronis, P. and H. K. Birnbaum (1995) *J. Mech. Phys. Solids* 43, 49.
4. Robertson I.M. and Birnbaum, H.K. (1986) *Acta Metall.* 34, 353.
5. Sofronis, P., Liang, Y. M. and Aravas, N. (2001) Submitted to *European Journal of Mechanics A: Solids*.
6. Tabata, T. and Birnbaum, H.K. (1983) *Scripta Metall.* 17, 947.
7. Oriani, R.A. (1970) *Acta Metall.* 18, 147.
8. Sofronis, P. and McMeeking, R.M. (1989) *J. Mech. Phys. Solids* 37, 317.
9. McMeeking, R.M. (1977) *J. Mech. Phys. Solids* 25, 357.